Skin Research and Technology 2013; **19**: 251–257
Printed in Singapore · All rights reserved
doi: 10.1111/srt.12034

Published by John Wiley & Sons Ltd
Skin Research and Technology

High-resolution multiphoton tomography and fluorescence lifetime imaging of UVB-induced cellular damage on cultured fibroblasts producing fibres.

Seidenari Stefania[1], Schianchi Simona[1], Azzoni Paola[1], Benassi Luisa[1], Borsari Stefania[1], Cautela Jennifer[1], Ferrari Chiara[1], French Paul[2], Giudice Stefania[1], Koenig Karsten[3], Magnoni Cristina[1], Talbot Clifford[2] and Dunsby Christopher[2]

[1]*Department of Dermatology, University of Modena and Reggio Emilia, Modena, Italy,*
[2]*Department of Physics, Imperial College London, Photonics Group, London, UK and* [3]*Department of Biophotonics and lasertechnology, Saarland University, Saarbruecken, Germany*

Background: Multiphoton tomography (MPT) is suitable to perform both ex vivo and *in vivo* investigations of living skin and cell cultures with submicron resolution. Fluorescence lifetime imaging (FLIM) generates image contrast between different states of tissue characterized by various fluorescence decay rates. Our purpose was to combine MPT and FLIM to evaluate fibroblasts and collagen fibres produced in vitro.
Methods: Fibroblast cultures, 2–4 days old, at a subconfluent stage, were evaluated before and after irradiation with a single UVB dose. One month old cultures stimulated with ascorbic acid were also assessed.
Results: After UVB radiation, fibroblasts appear irregular in size, lose their alignment and show a decrease in fluorescence lifetime. One month-old fibroblasts, producing collagen fibres after stimulation with ascorbic acid, appear as small roundish structures intermingled by filaments showing a granular arrangement.
Conclusion: The combination of MPT and FLIM may be useful for the in vitro study of cell modifications induced by injurious or protective agents and drugs.

Key words: multiphoton tomography – fluorescence lifetime imaging – extracellular – matrix – collagen – fibroblasts

Accepted for publication 10 November 2012

THE RECENT development of advanced non-invasive clinical imaging instruments has facilitated fast observation of the skin at high resolution, valuable both in laboratory research and clinical practice. One of the most recent clinical imaging technologies is multiphoton tomography (MPT), which is becoming established as the preferred method for image living cells with submicron resolution (1). MPT can exploit autofluorescence of intrinsic tissue fluorophores, thereby enabling functional and structural imaging of unstained biological tissue (1–8). Whereas, for conventional confocal fluorescence microscopy, fluorophores are excited by absorption of individual photons in the visible or ultraviolet spectrum, MPT excitation entails the simultaneous absorption of two or more photons of longer wavelength, usually in the near-infrared spectrum. This longer wavelength infrared radiation undergoes less scattering than visible light, thus facilitating high-resolution imaging deeper into biological tissue. Efficient MPT excitation usually requires ultrashort femtosecond laser pulses, which are also efficient in producing the nonlinear effect of second harmonic generation (SHG), engendered by periodic structures in tissue matrix components such as collagen (8). The combination of autofluorescence imaging and SHG gives access to morphology and structure of both cells and extracellular matrix of the skin (1–8). Fluorescence lifetime imaging (FLIM) is an additional technique based on the time-resolved analysis of the fluorescence signal enabling the non-invasive imaging of different states of tissue characterized by different fluorescence decay rates (9, 10).

UV radiation is directly related to the development of skin cancer and the carcinogenic effect is primarily attributed to the UVB portion of solar radiation (11–13). In response to UVB-induced damage, the cell can trigger cell-cycle arrest, providing time for DNA repair before replication or apoptosis. Induction of apoptosis following UV radiation can be a self-protective mechanism by which irreversibly damaged and potentially neoplastic cells are deleted. Moreover, both cell necrosis and apoptosis represent evaluation parameters considered in *in vitro* experiments assessing the toxicity or the protective capacity of different molecules. Fibroblasts represent the main cell population of the dermis generating the dermal extracellular matrix composed of glycosamino-glycans, reticular and elastic fibres, and glycoproteins. Cultured fibroblasts are often employed to study the cellular response to various chemical stimuli and to UV radiation. So far, fibroblasts' morphology has been evaluated mainly using optical microscopy; whereas to confirm the apoptotic process, fixation and staining procedures are necessary.

The aim of our study was to combine MPT and fluorescence lifetime imaging to evaluate fibroblasts and collagen fibres produced *in vitro*. Fibroblast cell cultures were assessed, before and after UVB-induced damage, for the identification of alterations of the morphology of single cells and nuclei and modifications of fluorescence lifetime decay rates suggestive of cell damage or apoptosis. Moreover, fibroblast cell cultures were grown for 1 month and treated with ascorbic acid to stimulate the production of collagen fibres, which were studied by means of MPT and FLIM.

Material and Methods

Cell cultures

Normal human fibroblasts were obtained after excision of skin specimens from neonatal foreskin. The skin was minced in small pieces, placed in a sterile tube and incubated for 12–18 h in a refrigerator (+4°C) in 2-ml dispase solution diluted in Hanks' Balanced Salt Solution. The epidermis was then separated from the dermis by pliers, and the dermis was transferred to a 35-mm Petri dish. Fibroblasts were isolated from the dermis by explant cultures. The dermis was first cut into tiny pieces (1-mm^2 section) and placed into the centre of a 25-cm^2 flask. Explant cultures were covered with Dulbecco's modified eagle's medium containing 10% foetal calf serum and fed twice weekly. Outgrowth cells were sub-cultured in a 25-cm^2 flask when cells reached 25–50% confluence. Fibroblasts were inoculated at a density of 18.000 cells/cm^2 into sterile closed cell chambers by a syringe, inserting the needle through the silicon ring via the lateral slots. The chamber, MiniCeM™-biopsy, JenLab GmbH (Fig. 1) consists of a silicon ring and two round glass cover slips, each 0.17-mm thick. The two components of the chamber are connected by a bayonet fitting that enables a rapid change of the internal chamber set. One needle was used for venting the air from the chamber and another for introducing cells. After introduction of cells, the needle was carefully withdrawn, so that the chamber was sterilely closed. While working with adherent cell cultures, it was necessary to incubate the chamber horizontally with the cover with the MiniCeM™ logo side up, so that the cell layer was on the cover slip facing the objective. After 2–4 days of incubation, especially when cell numbers and size were large enough to be seen under the optical microscope, investigations were performed with the multiphoton tomograph (*DermaInspect*®). It is necessary to examine the cells within 1 h as they need to be placed into the incubator (37°C, 5% CO_2) to survive. The MiniCeM™ is placed on the *in vitro* adaptor with a drop of oil on its surface, and the microscope stage is adjusted manually until the first cell layers appear. Figure 1 shows the MiniCeM™ chamber and its use on the DermaInspect *in vitro* adaptor stage. To study the effects of UVB radiation on fibroblasts, including the morphological aspects of this phenomenon, we irradiated the fibroblasts

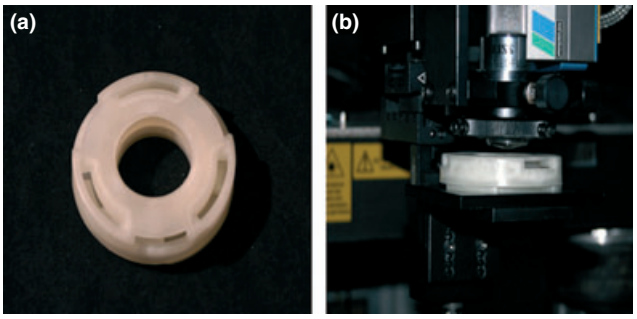

Fig. 1. The chamber employed for the growth and examination of cell cultures. b) the chamber containing the culture with the cover side up under the DermaInspect®.

with a single UVB dose of 300 mJ/cm^2 (14), using a UVB lamp (TL-20 Watt/12 RS Philips, Netherlands), which was calibrated by a Goldilux^{TM} smart meter (Oriel, Stratford, CT, U.S.A.). Fibroblast cell cultures were examined again at 24 h, 48 h and 7 days after UVB radiation. Control cultures not undergoing UVB irradiation were assessed only at baseline and at 48 h. Between examinations, cell cultures were put into the incubator. In total, we measured 6 samples, and for each sample, we performed 10 sequential MPT investigations and FLIM acquisitions before and after UVB irradiation. Fibroblasts were also seeded in a MiniCeM™ at a density of 125.000 cells/cm^2. Subsequently, ascorbic acid 250 μmol was added to the culture medium three times a week. After 1 month, when a transparent sheet comprising cells and fibres was produced within the culture, cell cultures were investigated for the presence of fibres by multiphoton tomography and FLIM. The transparent film formed by the cell culture was then embedded in paraffin and coloured according to the trichromic staining.

Instrumentation and elaboration of the data

Multiphoton tomography: In this study, we used the MPT *DermaInspect imaging system* ® (Jenlab GmbH, Jena, Germany), which provides intratissue scanning with subcellular spatial resolution (0.5 μm in lateral direction and 1–2 μm in the axial direction) (2, 3, 5, 6). The CE-marked and commercially available imaging tool is rated as a class 1 M device according to the European laser safety regulations and consists of three major modules: laser, scanning-detector unit and control module. The laser source utilizes a mode-locked, 80 MHz, Ti:S (titanium:sapphire) laser (Mai-Tai; Spectra Physics, Mountain View, CA, USA) with a tuning range of 710–920 nm, a 75-fs pulse width and a maximum laser power of 900 mW that is attenuated to a maximum of 50 mW at the sample. The scanning-detector unit consists of a photodiode for electronic triggering, beam expander, fast x–y galvoscanners, a 40× focusing objective (NA = 1.3 oil) as well as a photomultiplier tube (PMT) for intensity imaging. A colour-glass filter (Schott BG39, ELMSFORD, NY, USA) is employed in front of the PMT to block the scattered laser radiation light.

For selective imaging and spectral fluorescence lifetime measurements, an excitation wavelength of 760 nm was applied. The imaging depth was pinpointed to the cell culture layer. Laser power was attenuated to 30–40 mW at the sample and images were acquired within 8 s per frame.

Fluorescence lifetime imaging (FLIM): Fluorescence Lifetime Imaging (FLIM) was implemented in the DermaInspect® system using a time-correlated single photon counting (TCSPC) module with a temporal instrument response function of approximately 250 ps width. The emitted autofluorescence was spectrally selected by means of a short pass optical filter (Schott BG39) to protect the detector from scattered excitation light (PMH 100-1; Becker & Hickl GmbH, Berlin, Germany). False-colour lifetime maps of cell cultures were produced by assigning a colour according to its lifetime value to each pixel of the image. The FLIM images were calculated using the software SPCImage (Becker & Hickl GmbH). A single exponential decay fitting model was employed to obtain a mean fluorescence lifetime at each pixel, and a SPC-Image binning factor of 2 was used in the analysis. The final output of the FLIM analysis is a pseudocolour image where the colour scale encodes the fluorescence lifetime and image brightness encodes the fluorescence intensity. All images were displayed with a fluorescence lifetime range from red (0 ns) to blue (2000 ns).

A custom-written software package ('FLIM analysis assistant software' provided by the Photonics Group at Imperial College London) was used to calculate the mean fluorescence intensity and lifetime values for selected areas of interest such as the cytoplasm or the nucleus of single cells. For the processing of MPT images, a region of interest (ROI) of 100x100 μm^2 was selected in each field of view. Within this ROI, the total number of cells and cytoplasm and nucleus diameters were measured. For each fluorescence intensity and FLIM acquisition, average values calculated on five areas of interest were considered. After baseline assessment, cell cultures were evaluated again at 24 h, 48 h and 7 days after UVB irradiation.

Statistics

Values were obtained from 6 cultures. For each sample, we obtained 10 MPT/FLIM images at

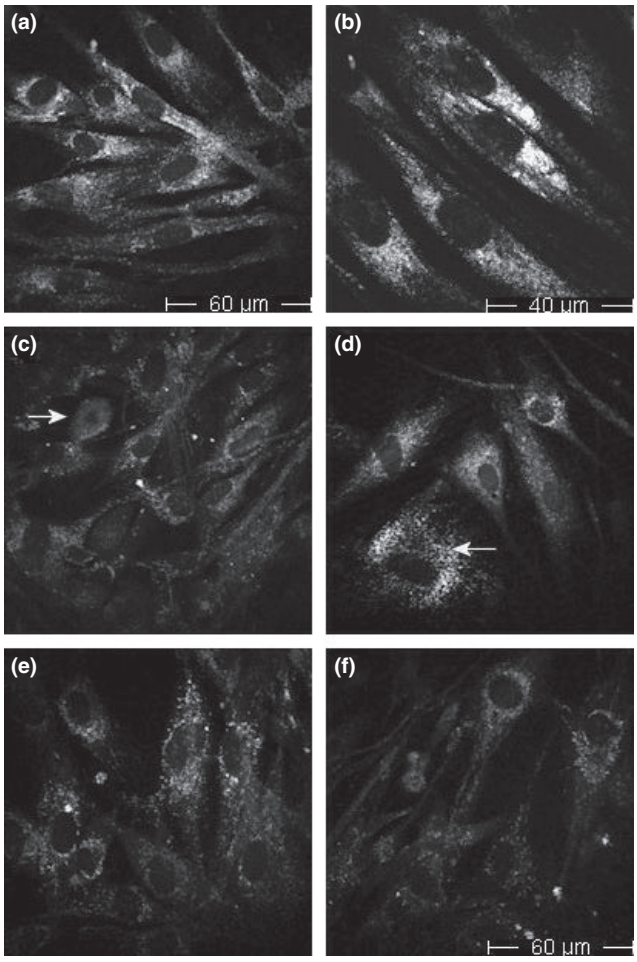

Fig. 2. MPT intensity images showing normal fibroblast cultures at 3 days post inoculation (a, b), and the morphologic alterations of fibroblasts after UVB exposure. Arrows indicate in (c) an apoptotic cell with a pyknotic nucleus, and in (d) a necrotic cell showing swelling and vacuolation of the cytoplasm 24 h after irradiation. (e, f) Cells 48 h after irradiation.

each time point and we measured cell diameter, nucleus diameter, number of cells and lifetime values from one area of interest per image (100 µm × 100 µm). Statistical examinations were performed with SPSS 12.0 for Windows (SPSS Inc., Chicago, IL, USA). Mean values and standard deviations were calculated for each considered parameter. Post-UV values were compared to those prior to UV radiation by means of the Mann–Whitney test. $P < 0.05$ was considered statistically significant.

Results

Morphology of cultured fibroblasts

In DermaInspect® images, fibroblasts appear as elongated cells with a big roundish nucleus, which, at culture confluence, are closely packed and aligned along the same axis (Fig. 2a, b). In some cases, the cytoplasm shows a uniform granular fluorescence, whereas in other cases, the fluorescent granular material is more asymmetrically distributed and mostly located around the nucleus. After UVB irradiation, cells appear irregular in size and lose their alignment (Fig. 2c–f). Some cells show a small nucleus and a condensation of the cytoplasm (Fig. 2c, arrow), which we believe correspond to apoptotic cells. In other cases, cells are larger than normal and show swelling and vacuolation of the cytoplasm (Fig. 2d arrow). Moreover, UVB-treated fibroblasts are oriented in several directions without a regular spatial organization and in some cases, their contours are blurred and difficult to recognize (Fig. 2e, f).

Quantitative data

Table 1 shows the results of the quantitative assessment of fibroblast cultures before and after UV radiation. At baseline, maximum diameter of fibroblast cells was ~130 µm and nucleus diameter was 20 µm; in a region of interest of 100 µm × 100 µm, we counted a mean of 18 cells. Average FLIM values of cytoplasm and nucleus were comparable (1180 ± 86 ps and 1136 ± 81 ps respectively). After UV irradiation, a decrease in the number of cells/ROI, in cell and nucleus size and an

TABLE 1. Quantitative assessment of cultured fibroblasts: cell and nucleus diameter and number of cells in a region of interest of 100 µm × 100 µm, and fluorescence lifetime values

	Before UVB-radiation	After UVB-radiation		
	Baseline	24 h	48 h	7 days
Ø cell (µm)	128.5 ± 25.9	94.9* ± 27.6	48.7* ± 16	44.8* ± 9.5
Ø nucleus (µm)	22.2 ± 3.31	21.6 ± 4.88	14.8* ± 3.5	16* ± 3.9
N° cells/ROI	18.4 ± 5.8	/	7.0* ± 1.2	/
average FLIM cytoplasm (ps)	1180.0 ± 86.1	/	1322.0* ± 63.0	/
average FLIM nucleus (ps)	1136.0 ± 81.1	/	1346.3 ± 87.5	/

Ø = diameter; ROI = region of interest; FLIM = fluorescence decay time in picoseconds (ps); * = significant with respect to baseline values.

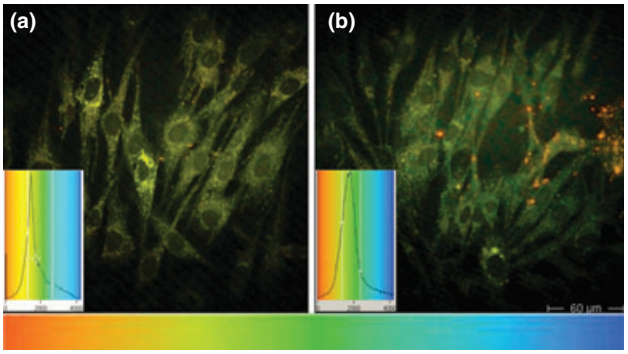

Fig. 3. FLIM images of fibroblasts before (a) and after (b) UVB radiation. The corresponding fluorescence lifetime histograms are also shown: a shift to the right of the post-UVB curve indicates an increase in fluorescence lifetime values. The colour bar represents the fluorescence lifetime on a scale of 0 (red) to 4000 (blue) ps.

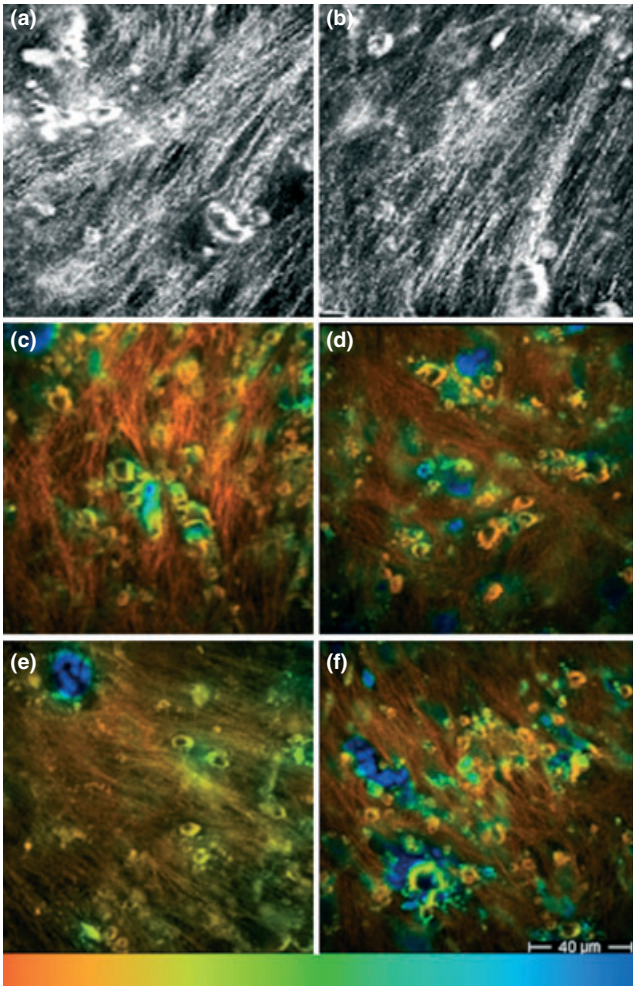

Fig. 4. Five week-old fibroblast cultures comprising cells and fibres. In intensity images (a and b) fibroblasts appear as small cells with a small nucleus, whereas collagen fibres are filamentous structures, where in some cases a granular arrangement is observable. In FLIM images (c-f) both cells and fibres show low FLIM values. The colour bar represents the fluorescence lifetime on a scale of 0 (red)–4000 (blue) ps.

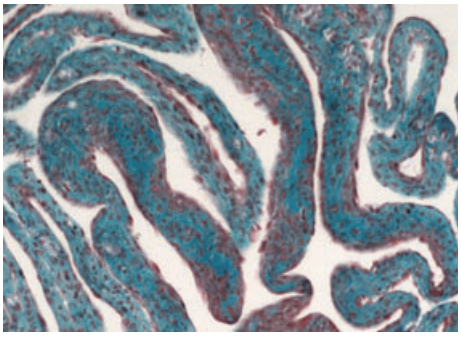

Fig. 5. Masson's trichrome staining of normal human fibroblasts stimulated with ascorbic acid. Collagen fibers appear blue-green, the cytoplasm pink and the nuclei dark brown.

increase in fluorescence lifetime was observed. The increase in fluorescence lifetime values is clearly apparent in the inset histogram of Fig. 3. Control MPT/FLIM experiments at 48 h showed no significant change in any of the assessed parameters.

When 1-month-old cultures, stimulated with ascorbic acid 250 µmol three times a week, were assessed, we imaged a continuous sheet comprising a mix of cells and fibres (Fig. 4). Fibroblasts appeared as small roundish structures with undefined borders, intermingled by filamentous collagen fibres showing a granular arrangement; in almost all cells, a small nucleus was recognizable. When performing the FLIM investigation, the fibres showed very short lifetimes, as expressed by the red and yellow colours of a 0–4000 colour scale. Masson's trichrome staining of these 1-month cell cultures showed the presence of collagen fibres coloured in blue-green, whereas cell cytoplasm appeared pink and cell nuclei dark brown (Fig. 5).

Discussion

Multiphoton tomography with FLIM enables imaging of endogenous fluorophores in the skin with submicron resolution, which can reveal detailed morphology of epithelial and dermal structures (1–8). The main endogenous fluorophores observed in the skin include the reduced coenzyme NAD(P)H, which emits in the blue/green spectral range with a maximum around 460 nm (15), oxidized flavoproteins, which emit in the green spectral region (15), lipofuscin, which emits in the yellow spectral region (16), and melanin, which emits in the green/yellow spectral region (17). The fluorescence signal can be complemented by the SHG signal that is

generated when collagen is irradiated with ultra-short NIR laser pulses (5, 8). For MPT/FLIM, image data are represented using a pseudocolour scale to encode fluorescence lifetime. This lifetime contrast permits different cell types (keratinocyte, melanocyte, fibroblast, etc) to be distinguished. As the aim of our study was to perform investigations on a single cell type, the fibroblast, it was decided to use cell cultures rather than tissue samples to simplify the analysis and interpretation. Cultured human fibroblasts also have an interest by themselves, as cell cultures are widely used as an experimental model in various types of investigations, to study of the effect of drugs, especially of new compounds with potential chemotherapeutic activity, and of mutagenic and carcinogenic substances. In addition, cell cultures are also employed to investigate the effect of expression of specific genes (18, 19). For studies of radiation-induced cell damage, the outcome is often evaluated by assessing the morphology of the fibroblasts using optical microscopy, whereas to confirm the apoptotic process, immunohistochemistry, fluorescence-activated cell sorting, western blot analysis or molecular biology are generally employed (20, 21). Using MPT and FLIM, a precise and rapid morphological assessment of the cells can be achieved without the need of cell processing and staining or the execution of other laboratory analyses. After exposure to UVB, we observed a reduction in mean cytoplasm and nucleus diameter as assessed in our culture samples. When evaluating the alterations of single cells, however, two different types of modified fibroblasts were observed: small roundish cells with a small nucleus, and large spongiotic fibroblasts with undefined contours. We note that cell death generally occurs via two different processes: necrosis and apoptosis. These forms of cell death involve different characteristic morphological changes. Necrotic cells are characterized by an overall increase in cellular size, followed by the rupture of the cell membrane and release of the cellular content, while apoptotic cells shrink in size and exhibit marked alterations in the chromatin structure at an early stage (22). The chromatin becomes highly condensed within the nucleus and can appear concentric with the nuclear membrane. As cell death is a stochastic process, apoptotic stimuli do not tend to induce death in the cells at precisely the same time, and therefore very few apoptotic cells will be detected when observing a cell culture or tissue section at a specific time after a damaging stimulus.

We also applied FLIM to fibroblast cell cultures before and after UVB irradiation. Baseline FLIM values of fibroblasts were similar to those observed in upper layer keratinocytes *in vivo* (23). We note that characterizing the fluorescence lifetime parameters of healthy fibroblasts may help in identifying fibroblasts in *ex vivo* and *in vivo* studies, when they are intermingled with other cell types. Following the induction of UVB damage to fibroblasts, we observed an increase in the mean fluorescence lifetime values of the cytoplasm and nuclei that we attribute to an altered metabolic activity in the cells, such as is expected before cell death (21). This is confirmed by the observation of a lengthening of FLIM values in keratinocytes of elderly subjects *in vivo* (23). Moreover, lower layer keratinocytes exhibit shorter lifetime values with respect to keratinocytes of the stratum corneum and the stratum granulosum. These data indicate that FLIM values may be inversely related to the metabolic activity of living cells.

One-month-old cultures stimulated with ascorbic acid exhibited the presence of both small old fibroblasts and fibres, the latter being predominant in some part of the culture. Newly produced collagen fibres appeared with pseudocolours corresponding to very low fluorescence lifetime values, which is likely due to the coexistence of short SHG signals and a component of collagen autofluorescence (9). Further work with spectrally resolved FLIM is needed to separate the contributions of SHG and autofluorescence. The identification of characteristic signatures of collagen fibres may prove useful for the study of skin diseases based on the pathological accumulation of fibres in the dermis.

To conclude, in this study, we have presented data on MPT-derived morphology and fluorescence lifetime parameters of a single cell type, the fibroblast, and observed the effects of UVB irradiation, which is the most potent environmental risk factor in skin cancer pathogenesis, on this cell. This approach for the evaluation of morphological and metabolic cell changes can be applied to the experimental assessment of the toxicity or the protective capacity of the

different drugs and substances. We also believe that the characterization of fibroblasts and fibroblast-produced fibres in culture is a useful precursor to the *in vivo* study of pathological cells in skin diseases based on the abnormal production and accumulation of dermal fibres.

References

1. Denk W, Strickler JH, Webb WW. Two-photon laser scanning microscopy. Science 1990; 248: 73–76.
2. König K, Riemann I. High-resolution multiphoton tomography of human skin with subcellular spatial resolution and picosecond time resolution. J Biomed Opt 2003; 8: 432–439.
3. Schenke-Layland K, Riemann I, Damour O et al. Two-photon microscopes and in vivo multiphoton tomographs - Powerful diagnostic tools for tissue engineering and drug delivery. Adv Drug Deliv Rev 2006; 58: 878–896.
4. 'Schenkl S, Weiss EC, Stracke F et al. In-vivo observation of cells with a combined high-resolution multiphoton-acoustic scanning microscope. Microsc Res Tech 2007; 70: 476–480.
5. König K. Clinical multiphoton tomography. J Biophotonics 2008; 1: 13–23.
6. Koehler MJ, Hahn S, Preller A et al. Morphological skin ageing criteria by multiphoton laser scanning tomography: non-invasive in vivo scoring of the dermal fibre network. Exp Dermatol 2008; 17: 519–523.
7. Tsai TH, Jee SH, Dong CY et al. Multiphoton microscopy in dermatological imaging. J Dermatol Sci 2009; 56: 1–8.
8. Wang BG, König K, Halbhuber KJ. Two-photon microscopy of deep intravital tissues and its merits in clinical research. J Microsc 2010; 238: 1–20.
9. Elson DS, Galletly N, Talbot C et al. Multidimensional Fluorescence Imaging Applied to Biological Tissue. Rev Fluores 2006; 3: 477–524.
10. Galletly NP, McGinty J, Dunsby C et al. Fluorescence lifetime imaging distinguishes basal cell carcinoma from surrounding uninvolved skin. Br J Dermatol 2008; 159: 152–161.
11. Oka M, Edamatsu H, Kunisada M et al. Enhancement of ultraviolet B-induced skin tumor development in phospholipase Cε-knockout mice is associated with decreased cell death. Carcinogenesis 2010; 31: 1897–1902.
12. Von Thaler AK, Kamenisch Y, Berneburg M. The role of ultraviolet radiation in melanomagenesis. Exp Dermatol 2010; 19: 81–88.
13. Koehler MJ, Preller A, Kindler N et al. Intrinsic, solar and sunbed-induced skin aging measured in vivo by multiphoton laser tomography and biophysical methods. Skin Res Technol 2009; 15: 357–363.
14. Rünger TM, Farahvash B, Hatvani Z, Rees A. Comparison of DNA damage responses following equimutagenic doses of UVA and UVB: a less effective cell cycle arrest with UVA may render UVA-induced pyrimidine dimers more mutagenic than UVB-induced ones. Photochem Photobiol Sci 2012; 11: 207–15.
15. Huang S, Heikal AA, Webb WW. Two-photon fluorescence spectroscopy and microscopy of NAD(P)H and flavoprotein. Biophys J 2002; 82: 2811–2825.
16. Haralampus-Grynaviski NM, Lamb LE, Clancy CM et al. Spectroscopic and morphological studies of human retinal lipofuscin granules. Proc Natl Acad Sci U S A 2003; 100: 3179–3184.
17. Teuchner K, Ehlert J, Freyer W et al. Fluorescence Studies of Melanin by stepwise two-photon femtosecond laser excitation. Journal of Fluorescence 2000; 10: 275–281.
18. Rossi T, Benassi L, Magnoni C et al. Effects of glycyrrhizin on UVB-irradiated melanoma cells. In Vivo 2005; 19: 319–322.
19. Giudice S, Benassi L, Bertazzoni G et al. New thymidylate synthase inhibitors induce apoptosis in melanoma cell lines. Toxicol In Vitro 2007; 21: 240–248.
20. Giudice S, Benassi L, Bertazzoni G et al. Biological evaluation of MR36, a novel non-polyglutamatable thymidylate synthase inhibitor that blocks cell cycle progression in melanoma cell lines. Invest New Drugs 2012; 30: 1484–92.
21. Raj D, Brash DE, Grossman D. Keratinocyte apoptosis in epidermal development and disease. J Invest Dermatol 2006; 126: 243–57.
22. Wang HW, Gukassyan V, Chen CT et al. Differentiation of apoptosis from necrosis by dynamic changes of reduced nicotinamide adenine dinucleotide fluorescence lifetime in live cells. J Biomed Opt 2008; 13: 054011.
23. Benati E, Bellini V, Borsari S et al. Quantitative evaluation of healthy epidermis by means of multiphoton microscopy and fluorescence lifetime imaging microscopy. Skin Res Technol 2011; 17: 295–303.

Address:
Luisa Benassi
Department of Dermatology
Policlinico, Via del Pozzo 71
University of Modena and Reggio Emilia
41124 Modena
Italy
Tel:+390594222935
Fax:+390594224271
e-mail: luisa.benassi@unimore.it